applied sciences

MDPI

Article

Study on the Evolution Law and the Orientation Criterion of a Plastic Zone in Rock Surrounding a Circular Roadway in a Three-Dimensional Non-Isobaric Stress Field

Hongtao Liu, Zijun Han *, Zhou Han, Xiaofei Guo, Tianhong Huo, Shengjie Wei, Zilong Luo and Jiquan Ma

School of Energy and Mining Engineering, China University of Mining and Technology (Beijing), Beijing 100083, China; 108925@cumtb.edu.cn (H.L.); hanzhou97@163.com (Z.H.); 15201290185@163.com (X.G.); hth@student.cumtb.edu.cn (T.H.); 18955499644@163.com (S.W.); sichuanlzl@163.com (Z.L.); cumtblove@163.com (J.M.)

* Correspondence: cumtbhzj@163.com; Tel.: +86-138-3416-9411

Abstract: The original rock stress field is mainly divided into the σ_{HZ}-dominant stress field, the σ_Z-dominant stress field, and the σ_H-dominant stress field. Via theoretical analysis, the plastic zone morphology and the orientation of roadway surrounding rock under a three-dimensional stress field are studied in depth, and the theory is verified by numerical simulation. The results show that in the σ_{HZ}-dominant stress field, the plastic failure mode changes from elliptical to quasi-circular to butterfly, and the optimized angle range of the roadway orientation is determined by three principal stresses. In the σ_Z-dominant stress field, the shape of the plastic zone transforms from butterfly to ellipse, the optimized angle range of the roadway orientation is 50–90°, and the butterfly hidden danger zone is in the 0–50° range. In the σ_H-dominated stress field, the shape of the plastic zone transits from ellipse to butterfly. The optimized angle range of the roadway orientation is 0–40°, and 50–90° is the butterfly hidden danger zone.

Keywords: ground stress; plastic zone morphology; butterfly destruction; roadway orientation; roofing

Citation: Liu, H.; Han, Z.; Han, Z.; Guo, X.; Huo, T.; Wei, S.; Luo, Z.; Ma, J. Study on the Evolution Law and the Orientation Criterion of a Plastic Zone in Rock Surrounding a Circular Roadway in a Three-Dimensional Non-Isobaric Stress Field. *Appl. Sci.* **2022**, *12*, 2947. https://doi.org/10.3390/app12062947

Academic Editors: Arcady Dyskin and Daniel Dias

Received: 4 February 2022
Accepted: 12 March 2022
Published: 14 March 2022

1. Introduction

In coal mine safety, the deformation and failure of roadway surrounding rock have been hot topics of research; the control of the plastic zone expansion of roadway surrounding rock is a problem that needs to be urgently solved. Ground stress is the main factor leading to the failure of roadway surrounding rock, and the original rock stress field is the basis for analyzing the stress redistribution of roadway surrounding rock. It is critical to study the roadway orientation under different stress fields for the stability of roadway surrounding rock [1,2].

Many in-depth studies have been conducted on the deformation mechanism and deformation characteristics of roadway surrounding rock [3–7]. Bagheri et al. deduced the boundary equation of the plastic zone of the surrounding rock of a circular roadway and established a two-dimensional numerical simulation model. The radius of the plastic zone was measured and analyzed by applying 13 stress states, helping to verify the theoretical analysis [8]. Xu et al. put forward the pressure relief method of slotting in the roof and floor of a roadway and studied the release effect of the slotting depth on the plastic zone by the Mohr–Coulomb criterion [9]. Hou et al. proposed the reasonable use of primary support and secondary support to achieve long-term stability of the roadway in view of floor heave and creep in the control of the surrounding rock of a deep roadway [10]. Ma et al. systematically used the two-dimensional distribution stress solution and Mohr–Coulomb strength theory in elastic–plastic mechanics to obtain the formula of deviatoric stress and the plastic zone radius of circular roadway surrounding rock under a non-uniform stress field and studied the distribution law of deviatoric stress and the plastic zone, providing a

reasonable theoretical basis for roadway support optimization [11]. Chen et al. systematically studied the deformation and failure characteristics of deep roadway surrounding rock and obtained the surrounding rock mechanics and strata behavior characteristics of a deep mining roadway [12]. Sun et al. studied the influence of horizontal stress on the stability of roadway surrounding rock [13]. Based on the space–time relationship of plastic zone expansion during repeated mining, Liu et al. revealed the mechanical mechanism of the space–time relationship of the plastic zone with the expansion of roadway surrounding rock and put forward the method of graded reinforcement [14]. Based on the plane strain problem, Zhao et al. proposed the butterfly failure theory of roadway surrounding rock; they clarified that roadway surrounding rock failure has three basic forms, circular, elliptical, and butterfly, and explained the physical phenomena of asymmetric large deformation and roof fall of the roadway [15]. Guo et al. proposed the concept of the shape coefficient of the plastic zone, deduced the formula of the shape coefficient, and used its size to distinguish the shape characteristics of the plastic zone, significant for roadway stability analysis and support design [16].

According to the maximum horizontal stress theory proposed by Australian scholars, roadway surrounding rock is most stable when the roadway axial direction is parallel to the maximum horizontal stress direction [17]. However, this theory has some problems. According to the butterfly failure theory of roadway surrounding rock, the principal stress ratio η of the regional stress field influences the stability of roadway surrounding rock. When the confining pressure ratio is large, a large stress deviation occurs in two directions, forming a high-deviatoric-stress environment, which creates conditions for the formation of a butterfly plastic zone. Once formed, this zone causes the large-scale destruction of roadway surrounding rock. At the same time, the failure zone is sensitive to stress change, which can easily cause dynamic disasters, such as floor heave, roof fall, large deformation, and rock burst [18]. In addition, the butterfly plastic zone has the support micro-effect. Under the existing support conditions, the support resistance of the roadway butterfly plastic zone control effect is limited.

Therefore, it is necessary to consider the influence of different roadway orientations in the ground stress field on the shape of the plastic zone of roadway surrounding rock to avoid as much as possible the formation of a high-deviatoric-stress-difference environment, in line with the actual conditions of the project. A reasonable orientation range will ensure that the roadway is in the low confining pressure ratio range so that the plastic zone of the surrounding rock is round or oval, not butterfly. This will help avoid difficult support, high support cost, serious roof fall, and a series of other problems. In this paper, under the guidance of the butterfly failure theory of roadway surrounding rock, through theoretical analysis and numerical simulation, the evolution law of the plastic zone in rock surrounding a circular roadway with different orientations under different stress fields is studied, the stability of roadway surrounding rock is analyzed, and the guiding role of engineering is put forward based on theoretical analysis, which provides a theoretical basis for orientation optimization layout and roadway safety.

2. Theoretical Analysis of the Plastic Zone under a Non-Isobaric Stress Field

2.1. General Form of the Plastic Zone in Rock Surrounding a Circular Roadway

In coal mining, roadway layout, stope strata control and movement, roadway strata behavior control, and the coal mine dynamic pressure phenomenon are closely related to the crustal stress field. The size and direction of original rock stress largely affect roadway deformation and failure. Therefore, it is important to study the initial stress field environment of a roadway to analyze the internal stress change of a rock mass during excavation and design reasonable support.

The schematic diagram of roadway surrounding rock under a three-dimensional stress environment is shown in Figure 1.

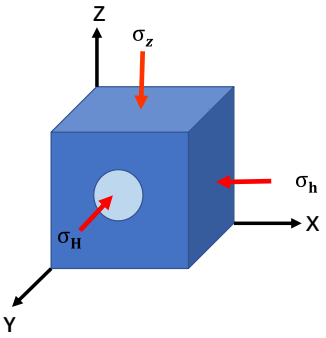

Figure 1. Schematic diagram of the stress field environment in the roadway envelope.

In Figure 1, σ_H is the maximum horizontal principal stress, parallel to the roadway axis; σ_h is the minimum horizontal principal stress, perpendicular to the roadway side; and σ_Z is the vertical stress.

In the existing research, the actual roadway model can be simplified into the axisymmetric plane strain circular hole problem in elastoplastic mechanics. The mechanical model is shown in Figure 2, where P_1 is the principal stress of the side of the vertical roadway, P_3 is the direct lead stress, a is the radius of the roadway, r and θ are the polar coordinates of any point in the coordinates, and η is the confining pressure ratio (i.e., the ratio of the main stress of two sides of the vertical roadway to the vertical stress of the roadway). The expression is shown in Equation (1):

$$\frac{|P_1|}{|P_3|} = \eta \geq 1 \tag{1}$$

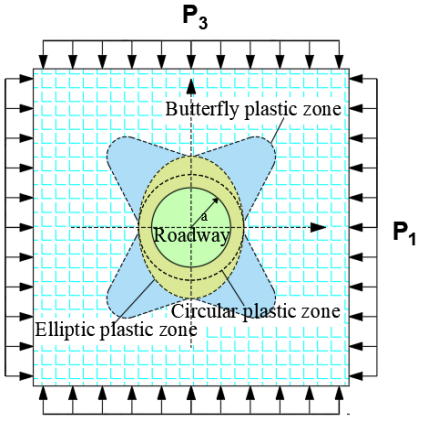

Figure 2. Mechanical calculation model and plastic zone evolution model of a circular roadway under a non-uniform stress field.

Through the stress analysis of a circular roadway under a non-uniform stress field, the stress calculation formula of any point around the roadway under non-uniform pressure is substituted into the Mohr–Coulomb criterion, the 8-order implicit equation of the plastic zone boundary of the surrounding rock of a circular roadway under a non-uniform stress field is obtained, as shown in Equation (2), and the concept of the butterfly plastic zone is proposed [19].

$$f\left(\frac{a}{r}\right) = K_1\left(\frac{a}{r}\right)^8 + K_2\left(\frac{a}{r}\right)^6 + K_3\left(\frac{a}{r}\right)^4 + K_4\left(\frac{a}{r}\right)^2 + K_5 = 0 \tag{2}$$

where

$$K_1 = 9(1-\eta)^2$$
$$K_2 = -12(1-\eta)^2 - 6\left(1-\eta^2\right)\cos 2\theta$$
$$K_3 = 2(1-\eta)^2\left[\cos^2 2\theta\left(5+2\sin^2\varphi\right) - \sin^2 2\theta\right] + (1+\eta)^2 + 4\left(1-\eta^2\right)\cos 2\theta$$
$$K_4 = -4(1-\eta)^2\cos 4\theta - 2\left(1-\eta^2\right)\cos 2\theta\left(1+2\sin^2\varphi\right) + \frac{4}{\gamma H}(1-\eta)\cos 2\theta\sin 2\varphi C$$
$$K_5 = (1-\eta)^2 - \sin^2\varphi\left(1+\eta+\frac{2C\cos\varphi}{\gamma H\sin\varphi}\right)^2$$

where C is for coal and rock medium cohesion, a is the internal friction angle, r is the roadway radius, f is the radius of the plastic zone, and K is for the polar coordinates of any point around the roadway surrounding rock.

When η = 1, Equation (2) is the same as the famous Kastner formula. The plastic zone morphology of circular roadway surrounding rock under different η values under the same mechanical properties as those of roadway surrounding rock is obtained through Equation (2) and visual programing calculation, as shown in Figure 3. In the diagram, the plastic zone in the rock surrounding the circular roadway has three forms: circular, elliptical, and butterfly [20].

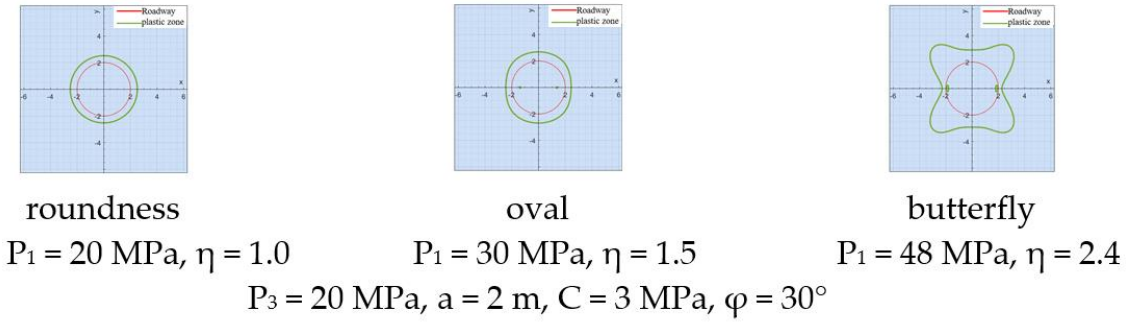

Figure 3. Theoretical calculation results of the butterfly plastic zone in the rock surrounding a circular roadway.

When the roadway plastic zone is circular and elliptical, the failure of the surrounding rock of the roadway is mostly uniform, the rock in the failure zone is not concentrated in a certain area, and the surrounding rock of the roadway is relatively stable. When the roadway plastic zone is butterfly shaped, the failure of the surrounding rock of the roadway is non-uniform. The rock in the failure zone is equivalent to the concentrated compression of the surrounding rock of the weak body. If the support is improper, roof fall accidents can easily occur, and the stability of the surrounding rock of the roadway is poor.

In the process of roadway axial rotation, the confining pressure of different angles varies greatly. When the stress difference is large, a high-deviatoric-stress environment is formed, creating stress conditions for the formation of a butterfly plastic zone. According to the stress conditions and mechanical mechanism of the butterfly plastic zone, the confining pressure in different axial directions of roadways is analyzed to further determine whether the roadways in different axial directions are in the stress conditions of a butterfly plastic zone, and the plastic zone morphology of different roadway orientations under different dominant stress fields is further analyzed.

2.2. Theoretical Analysis of Optimization Orientation of Roadway Surrounding Rock

In the three dominant stress fields, σ_{HZ}, $\sigma_{Z,}$ and σ_H, by calculating the change in the surrounding rock stress under different orientations of roadway, combined with the butterfly failure theory of roadway surrounding rock, the influence of angle α between the roadway axial direction and the maximum horizontal principal stress direction on

the stability of the roadway surrounding rock is analyzed to determine the reasonable excavation direction of the roadway.

In the initial stress field, it is assumed that the complex stress field around the roadway is represented by the regional main stress field, such as Equations (3)–(5):

$$\sigma_Z = \gamma H = S_{zz} \tag{3}$$

$$S_{xx} = \sigma_h, S_{yy} = \sigma_H \tag{4}$$

$$\frac{S_{xx}}{S_{zz}} = \frac{\sigma_h}{\sigma_Z} = \eta \tag{5}$$

where γ is the rock bulk density (2.5 kN/m^3); h is the depth of the roadway, m; and S_{xx}, S_{yy}, and S_{zz} are normal stresses in the X, Y, and Z directions, respectively.

Figure 4 shows the stress analysis when the roadway rotates at a certain angle. The maximum horizontal principal stress σ_H is parallel to the y-axis, the minimum horizontal principal stress σ_h is parallel to the x-axis, and the vertical stress σ_Z is parallel to the z-axis. The roadway is assumed to be arranged along the y-axis, and the initial axial direction of the roadway is parallel to the direction of the maximum horizontal principal stress. α is the rotation angle of the roadway, that is, the angle between the direction of the maximum horizontal principal stress and the axial direction of the roadway; S'_{xx} is the stress perpendicular to the sidewall of the roadway; and S'_{yy} is the stress parallel to the axial direction of the roadway.

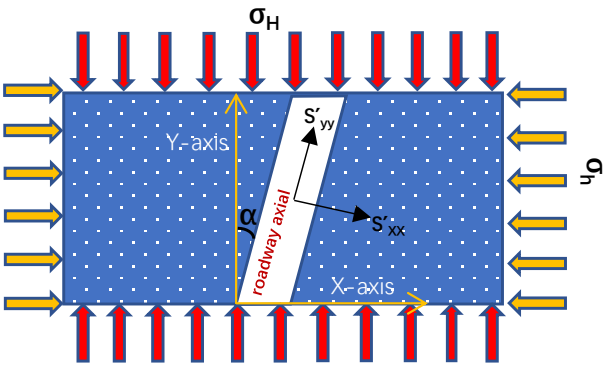

Figure 4. The stress analysis chart of the roadway after an axial rotation at α angle.

Through the stress analysis of the plane stress state of the unit body, the equilibrium equation is listed according to the known stress components on each surface of the unit body. Combined with the reciprocal theorem of shear stress [21], the expressions of S'_{xx}, S'_{xy}, and S'_{xy} are obtained as Equations (6)–(8):

$$S'_{xx} = \sigma_h \cos^2 \alpha + \sigma_H \sin^2 \alpha = \frac{\sigma_h + \sigma_H}{2} + \frac{\sigma_h - \sigma_H}{2} \cos 2\alpha \tag{6}$$

$$S'_{yy} = \sigma_H \cos^2 \alpha + \sigma_h \sin^2 \alpha = \frac{\sigma_h + \sigma_H}{2} + \frac{\sigma_H - \sigma_h}{2} \cos 2\alpha \tag{7}$$

$$S'_{xy} = \sigma_h \cos \alpha \sin \alpha - \sigma_H \cos \alpha \sin \alpha = \frac{\sigma_h - \sigma_H}{2} \sin 2\alpha \tag{8}$$

According to the butterfly failure theory of roadway surrounding rock and the stress state of the surrounding rock with different orientations, the roadway orientation schemes under three dominant stress fields are analyzed.

2.2.1. Optimal Orientation Theory Analysis of the σ_{HZ}-Dominant Stress Field

In the σ_{HZ} stress field, $\sigma_H > \sigma_Z > \sigma_h$. It can be seen from Equation (6) that with the increase in the axial angle α, cos2α monotonically decreases and the stress S'_{xx} of the

corresponding vertical roadway side monotonically increases. In the process of increasing, at one point, angle $S'_{xx} = \sigma_Z$ and then S'_{xx} continues to increase to become equal to the axial stress σ_H. In the σ_{HZ}-dominant stress field, there are four stress environments: (1) If the difference between $|\sigma_H - \sigma_Z|$ and $|\sigma_Z - \sigma_h|$ is small, it shows that the difference between S'_{xx} and σ_Z is not significant during the rotation of the roadway, and the ratio of high confining pressure is not formed, which is not favorable to the formation of a butterfly plastic zone. (2) If the difference between $|\sigma_H - \sigma_Z|$ and $|\sigma_Z - \sigma_h|$ is large, the difference between S'_{xx} and σ_Z is large, at 0° and 90°. The roadway is in a high-stress-ratio environment and the stress environment is in a high–low–high state in the axial rotation process. A certain angle range in the rotation process is conducive to avoiding the formation of a butterfly plastic zone. (3) If the difference between $|\sigma_H - \sigma_Z|$ is large and the difference between $|\sigma_Z - \sigma_h|$ is small, the difference between S'_{xx} and σ_Z is small at 0°, and the roadway is in a low-stress environment. With the increase in the distance to σ_H, the stress difference gradually increases, and a deviatoric stress area begins to form. (4) If the difference between $|\sigma_H - \sigma_Z|$ is small and the difference between $|\sigma_Z - \sigma_h|$ is large, the difference between S'_{xx} and σ_Z is large at 0°, and there is a high-stress difference, making it easy for a butterfly plastic zone to develop. With the increase in α, the deviatoric stress difference gradually decreases. In short, in the σ_{HZ}-dominant stress field, there is an angle α, which makes S'_{xx} equal to σ_Z and minimizes the deviatoric stress difference.

Take $\eta = \frac{S'_{xx}}{\sigma_Z} = 1$ into Equation (6) to obtain Equation (9):

$$\alpha = \frac{1}{2}\arccos\left(\frac{2\sigma_Z - \sigma_h - \sigma_H}{\sigma_h - \sigma_H}\right) \tag{9}$$

This α is the optimal angle deduced from the butterfly failure theory of roadway surrounding rock to avoid the formation of a butterfly plastic zone. The adjacent range of this angle is the optimal orientation. In this range, the plastic zone is elliptical or quasi-circular, which is conducive to the stability of the roadway.

2.2.2. Optimal Orientation Theory Analysis of the σ_Z-Dominant Stress Field

In the σ_Z stress field, $\sigma_Z > \sigma_H > \sigma_h$. It can be inferred from Equation (6) that as the roadway axial angle α increases, cos2α monotonically decreases and S'_{xx} monotonically increases. As angle α increases, S'_{xx} increases from σ_h to σ_H. In the σ_Z-dominant stress field, there are four stress environments: (1) If the difference between $|\sigma_Z - \sigma_H|$ and $|\sigma_H - \sigma_h|$ is small, the roadway does not produce an excessive deviatoric stress difference in the rotation process, and the butterfly failure zone is not formed. (2) If the difference between $|\sigma_Z - \sigma_H|$ and $|\sigma_H - \sigma_h|$ is large, the roadway is in a high confining pressure ratio environment when the roadway is 0°. With the increase in the axial angle α of the roadway, the deviatoric stress difference gradually decreases. Although there is a butterfly risk when the angle α is 90°, the risk is much lower than that of 0°. (3) If the difference between $|\sigma_Z - \sigma_H|$ is large and the difference between $|\sigma_H - \sigma_h|$ is small, the butterfly risk gradually decreases with the increase in angle α when the roadway transits from 0° to 90°. (4) If the difference between $|\sigma_Z - \sigma_H|$ is small and the difference between $|\sigma_H - \sigma_h|$ is large, the stress difference between S'_{xx} and σ_Z decreases rapidly with the increase in angle α during the rotation of the roadway, and the butterfly risk is greatly reduced, preventing the formation of a butterfly plastic zone. In conclusion, in the σ_Z stress field, with an increase in the axial angle α, when the angle range is small, the high confining pressure ratio environment is more likely to form, and the probability of butterfly risk greatly increases.

2.2.3. Optimal Orientation Theory Analysis of the σ_H-Dominant Stress Field

In the σ_H stress field, $\sigma_H > \sigma h > \sigma_Z$. It can be seen from Equation (6) that with the increase in the axial angle α of the roadway, cos2α decreases monotonically and the stress S'_{xx} corresponding to the vertical roadway sidewall increases monotonically. As angle

α increases, S'_{xx} transits from σ_h to σ_H. In the σ_{HZ}-dominant stress field, there are the following four stress environments: (1) If the difference between $|\sigma_H - \sigma_h|$ and $|\sigma_h - \sigma_Z|$ is small, in the process of roadway rotation, the stress difference between S'_{xx} and σ_Z is small. With the increase in the axial angle α of the roadway, the deviatoric stress difference of the surrounding rock of the roadway gradually increases but the high confining pressure ratio environment is not formed. (2) If the difference between $|\sigma_H - \sigma_h|$ and $|\sigma_h - \sigma_Z|$ is large, when the roadway is at 0°, the difference between S'_{xx} and σ_Z is large and the deviatoric stress difference continues to increase with the increase in angle α, rapidly increasing the risk of butterfly malignant plastic zone formation. (3) If the difference between $|\sigma_H - \sigma_h|$ is large and the difference between $|\sigma_h - \sigma_Z|$ is small, the difference in the stress of roadway orientation in the low-angle range is small and the butterfly risk coefficient increases with the increase in the roadway angle. (4) If the difference between $|\sigma_H - \sigma_h|$ is small and the difference between $|\sigma_h - \sigma_Z|$ is large, then there is a high-deviatoric-stress environment in the roadway at 0°. With the increase in the angle, the butterfly risk will continue to increase as in situations (2) and (3). In short, in the σ_H-type stress field, with an increase in the roadway angle, when the angle range is large, the high confining pressure ratio environment is easier to form, and the probability of butterfly risk also increases greatly.

2.3. Morphological and Size Characteristics of Theoretical Plastic Zones with Different Orientations under Three Dominant Stress Fields

According to the above three different dominant stress fields, the plastic zone boundary in Equation (1) under the condition of a non-uniform stress field is used to theoretically analyze the distribution characteristics and geometric forms of the plastic zone of a surrounding rock in the 0–90° range under the three stress fields. Under three dominant stress fields, each stress field gives a set of stress values, and the shape and size of the plastic zone are preliminarily determined by the equation.

In a σ_{HZ}-dominant stress field, when σ_H = 20 MPa, σ_Z = 8 MPa, and σ_h = 7 MPa, the shape of the plastic zone is shown in Table 1a. With the increase in the roadway angle α, the plastic zone morphology of the roadway surrounding rock transits from ellipse to quasi-circular to butterfly. In addition, the maximum sizes of the roadway plastic zone from 0° to 90° are 0.47, 0.46, 0.5, 0.68, 0.85, 1.06, 1.5, 2.15, 2.74, and 2.98 m, respectively, and the difference between the maximum plastic zone size and the minimum plastic zone size is 2.52 m.

Table 1. Theoretical analysis of plastic zone morphology with different orientations under three dominant stress fields.

									
α = 0°	α = 10°	α = 20°	α = 30°	α = 40°	α = 50°	α = 60°	α = 70°	α = 80°	α = 90°
(a) σ_{HZ}-dominant stress field									
									
α = 0°	α = 10°	α = 20°	α = 30°	α = 40°	α = 50°	α = 60°	α = 70°	α = 80°	α = 90°
(b) σ_Z-dominant stress field									
									
α = 0°	α = 10°	α = 20°	α = 30°	α = 40°	α = 50°	α = 60°	α = 70°	α = 80°	α = 90°
(c) σ_H-dominant stress field									

In the σ_Z-dominant stress field, with σ_H = 18 MPa, σ_Z = 20 MPa, and σ_h = 7 MPa, the shape of the plastic zone is shown in Table 1b. With the increase in the roadway angle α, the plastic zone morphology of the roadway surrounding rock transits from butterfly to ellipse. In addition, the maximum sizes of the roadway plastic zone from 0° to 90° are 4.37, 3.85, 2.69, 1.75, 1.34, 1.18, 1.12, 1.09, 1.07, and 1.06 m, respectively. The difference between the maximum plastic zone size and the minimum plastic zone size is 3.31 m.

In σ_H-dominant stress field, with σ_H = 20 MPa, σ_Z = 8 MPa, and σ_h = 9 MPa, the shape of the plastic zone is shown in Table 1c. With the increase in the roadway angle α, the plastic zone morphology of the roadway surrounding rock transits from ellipse to butterfly. In addition, the maximum sizes of the roadway plastic zone from 0° to 90° are 0.56, 0.55, 0.57, 0.72, 0.87, 1.03, 1.29, 1.66, 2.01, and 2.15 m, respectively. The difference between the maximum plastic zone size and the minimum plastic zone size is 1.60 m.

3. Numerical Simulation Analysis

3.1. Model Establishment

In this paper, a numerical model of 50 m × 22 m × 50 m (length × width × height) is established. The model has 660,000 elements, as shown in Figure 5. It adopts a unified lithology. The physical and mechanical parameters of rock strata are shown in Table 2, where the *x*-axis is the direction of the minimum horizontal principal stress, the *y*-axis is the direction of the maximum horizontal principal stress, and the *z*-axis is the direction of the lead direct stress. The front, rear, left, and right sides of the model are set as a horizontal displacement boundary, the bottom is set as a vertical displacement boundary, and the top is set as a stress boundary. The Mohr–Coulomb model is adopted.

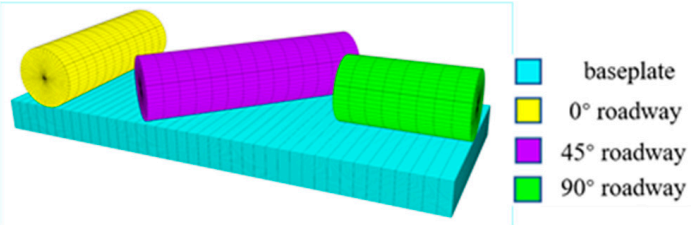

Figure 5. Numerical simulation model.

Table 2. Physical and mechanical parameters of rock formation.

Rockiness	Density/kg·m^{-3}	Tensile/MPa	Bulk/GPa	Shear/GPa	Cohesion/MPa	Friction/(°)
Coal	2400	0.35	14.17	9.33	3	25

3.2. Simulation Scheme

The simulation is carried out under three different stress fields. The boundary loading conditions under the three stress fields are consistent with the theoretical calculation, as shown in Figure 6. Under the three stress fields, the angle between the roadway axial direction and the direction of the maximum horizontal principal stress starts from 0° and rotates 10° clockwise each time. When the angle is 90°, that is, the maximum horizontal principal stress is perpendicular to the roadway side, the simulation stops. Ten groups of numerical models were established under each stress field, and the hist command was used to monitor the roof, side, and floor of the roadway.

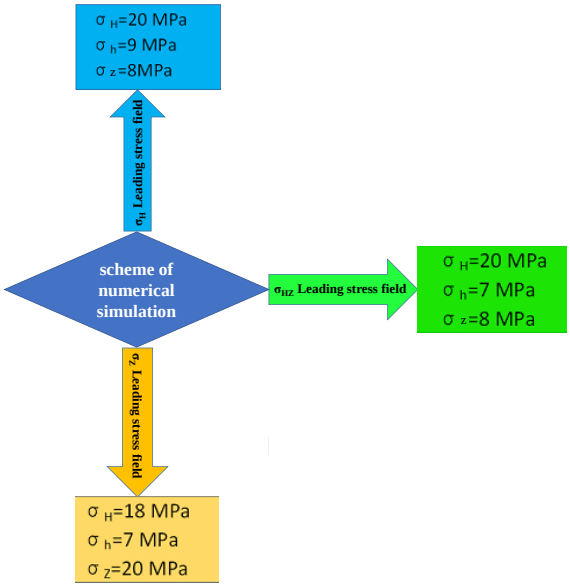

Figure 6. Boundary loading conditions under three stress fields.

3.3. Numerical Simulation Results and Analysis

The formation, development, and evolution of the surrounding rock plastic zone are the basis of the roadway surrounding rock deformation and failure. The morphological characteristics and distribution law of the plastic zone of surrounding rock are closely related to the stability of surrounding rock and the failure mode of a roadway. Only by fully understanding the evolution law and distribution characteristics of plastic zones in different roadway axial directions can a reasonable optimization scheme be made for the roadway layout so as to avoid the formation of a butterfly plastic zone morphology, which causes greater dynamic disasters. In this section, the evolution law of the plastic zone in different orientations of the roadway under three dominant stress fields is studied from the point of view of two core elements, plastic zone morphology and size, in different axial directions of the roadway.

3.3.1. Evolution Characteristics of the Plastic Zone under the σ_{HZ}-Dominant Stress Field

Figure 7 shows the distribution pattern of the plastic zone when angle α between the axial direction of the roadway and the direction of the maximum horizontal principal stress varies from 0° to 90° under the dominant stress field of σ_{HZ}. When the axial direction of the roadway is parallel to the maximum horizontal principal stress, the plastic zone of the surrounding rock of the roadway is quasi-circular. With the increase in the axial angle α of the roadway, the area of the two sides of the roadway decreases significantly and the area of the roof and the floor increases gradually. The plastic zone gradually transits from quasi-circular to vertical elliptical, and the area of the roof and the floor is much larger than that of the two sides. When α starts from 60°, the plastic zone size of roadway surrounding rock begins to develop obliquely and the butterfly shape is slowly revealed. The plastic zone of the roadway roof and floor continues to expand. When α is 90°, the plastic zone shape of the roadway is transverse butterfly.

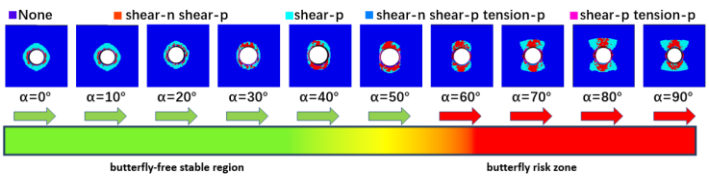

Figure 7. Distribution pattern of the roadway plastic zone under different values of angle α under the dominant stress field of σ_{HZ}.

Figure 8 shows the variation curve of the plastic zone size of the roadway with the axial angle α of the roadway. The following can be seen from the curve:

(1) When α is 0~60°, the maximum plastic zone size of the roadway occurs in the middle of the roof, and when α is 60~90°, the maximum plastic zone size of the roadway surrounding rock occurs at the wing angle.

(2) When α = 0°, the plastic zone at the roadway wing angle is 2.21 m. When α is 0~40°, the depth of the wing angle decreases by 0.83 m. When α is 40–90°, the size of the wing angle begins to increase rapidly and the sizes of the plastic zone are 1.38, 1.74, 2.06, 3.12, 4.04, and 4.40 m, respectively, increasing by 2.19 times.

(3) The depth of the plastic zone in the middle of the roof gradually decreases from 2.50 to 1.49 m when α increases from 0° to 40°, a decrease of 1.01 m. In the 50~90° range, the size of the plastic zone in the middle of the roof gradually increases, by 0.77 m.

(4) When the axial angle α of the roadway is in the 0~70° range, the size of the plastic zone in the middle of the roadway sidewall gradually decreases from 2.00 to 0.25 m, a decrease of 1.75 m or by 0.88 times. When α is 80~90°, the size of the plastic zone in the middle of roadway the sidewall slowly increases by 0.25 m.

(5) In the σ_{HZ}-dominant stress field, when the axial angle α of the roadway increases, the variation slope of the wing angle plastic zone size is the largest, followed by the roof, and the roadway side is the smallest. Therefore, in the σ_{HZ}-dominant stress field, the sensitivity of different positions of roadway to angle α is wing angle > roof > side.

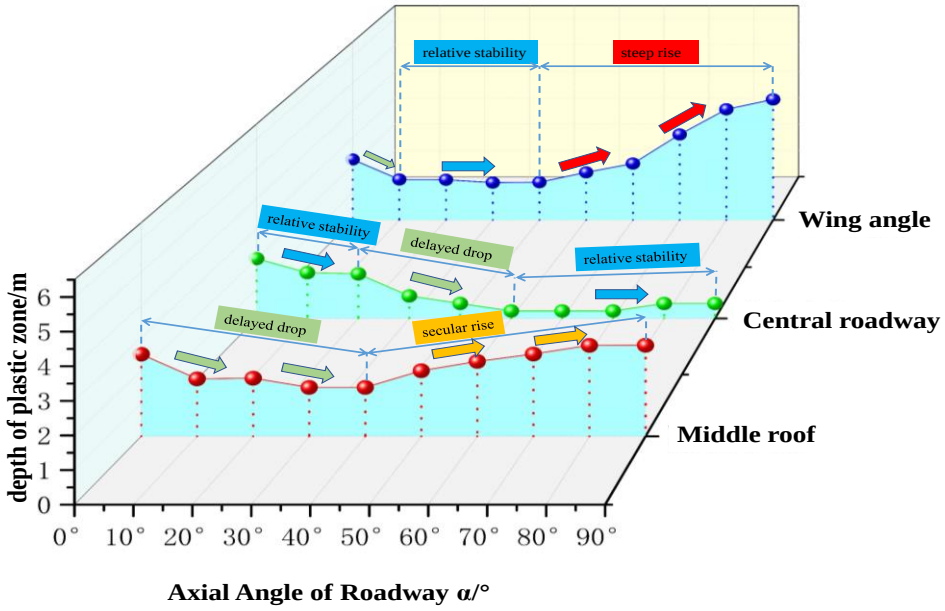

Figure 8. Variation in the depth of the plastic zone with axial angle α.

3.3.2. Evolution Characteristics of the Plastic Zone under a σ_Z-Dominant Stress Field

Figure 9 shows the distribution pattern of the plastic zone under the σ_Z-dominant stress field when the angle α between the roadway axial direction and the maximum horizontal principal stress direction changes between 0° and 90°. When α is 0°, the plastic zone in rock surrounding the circular roadway is an irregular vertical butterfly shape. With an increase in the axial angle of the roadway α, the wing angle of the roadway begins to decrease. When α is 50°, the butterfly shape of the roadway plastic zone is not obvious. The area of the two sides of the roadway is significantly larger than the area of the roof and the floor, which is similar to the flat ellipse. When α is 60–90°, the area of the plastic zone of the roof and the floor of the roadway surrounding rock increases gradually, and the plastic zone is close to a ring in shape.

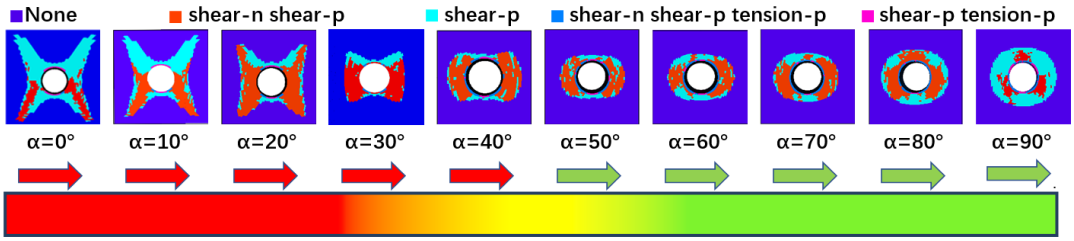

Figure 9. Distribution pattern of the roadway plastic zone under different values of angle α under the dominant stress field of σ_Z.

Figure 10 shows the variation curve of the plastic zone size of the roadway with the axial angle α of the roadway. The following can be seen from Figure 11:

(1) When α = 0°, the maximum size of the plastic zone of roadway surrounding rock occurs at the wing angle and the plastic zone size is 10.71 m, i.e., 3.57 times that of the roadway radius (3.57 a). With the increase in the axial angle α of the roadway (10~40°), the failure depth at the wing angle decreases sharply, and the failure radii are 9.12, 6.90, 4.39, and 3.00 m (i.e., decreases by 1.18, 1.55, 2.44, and 3.57 times, respectively). When α is 40–70°, the shoulder size is in a relatively stable stage, only decreasing by 0.4 m. When α is 80–90°, the plastic zone size of the roadway slowly increases by 0.86 m.

(2) With the increase in the roadway axial α (0~40°), the plastic zone size of the roadway roof decreases from 1.28 to 0.42 m, a decrease by 3.04 times. When α is 40~90°, the plastic zone depth slowly increases, from 0.42 to 2.78 m, increasing by 2.36 m.

(3) When the roadway axial angle α increases from 0° to 70°, the size of the plastic zone in the middle of the roadway sidewall does not change, and the size of the plastic zone is roughly 3 m. When α increases from 70° to 90°, the size of the plastic zone in the sidewall increases from 3 to 3.8 m, an increase of 0.8 m.

(4) In the process of axial rotation of the roadway, when α is between 0° and 40°, the maximum plastic zone depth of the roadway occurs at the roadway wing angle, and from 50°, the maximum failure depth of the roadway occurs at the roadway side.

(5) In the three positions of the roadway roof, sidewall, and four wings, as the roadway axial angle α increases, the curve slope of the wing angle changes the most, followed by the change in the roof, and the slope of the sidewall changes the least. Therefore, in the σ_Z-dominant stress field, the sensitivity of different positions of the roadway to angle α is wing angle > roof > side.

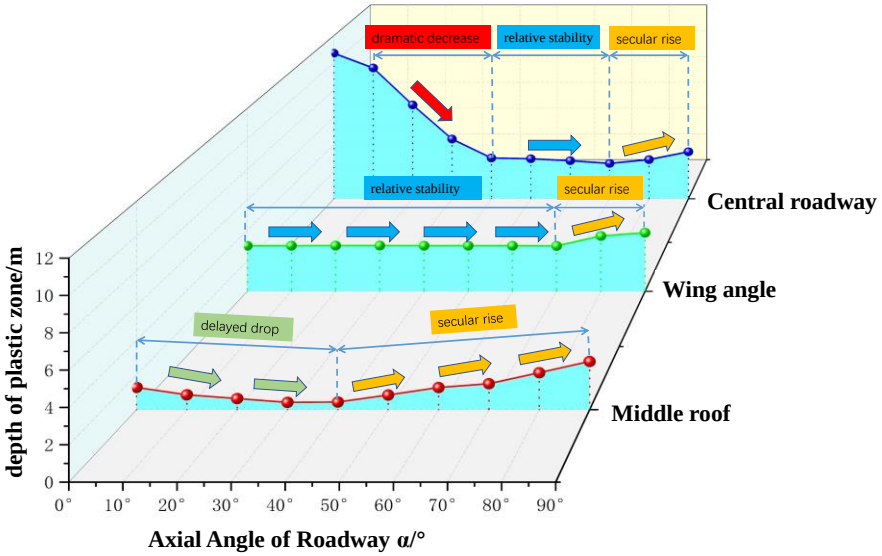

Figure 10. Variation in the depth of the plastic zone with axial angle α.

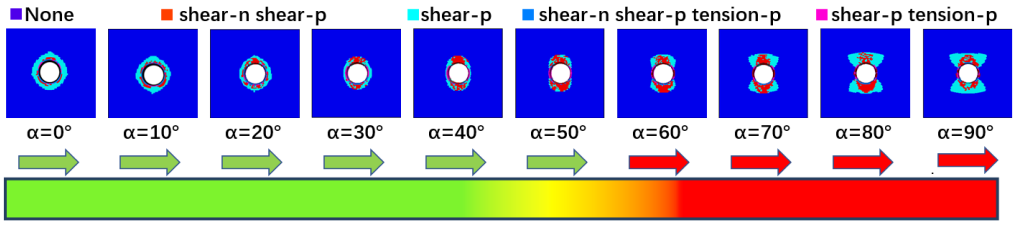

Figure 11. Distribution pattern of the roadway plastic zone under different values of angle α under the dominant stress field of σ_H.

3.3.3. Evolution Characteristics of the Plastic Zone under a σ_H-Dominant Stress Field

Figure 11 shows the distribution pattern of the plastic zone under the σ_H-dominated stress field when the angle α between the roadway axial direction and the maximum horizontal principal stress direction changes between 0° and 90°. When α is 0°, the plastic zone morphology of roadway surrounding rock is quasi-circular and the plastic zone is evenly distributed around the roadway. With an increase in the axial angle of the roadway (10~50°), the plastic zone area of the two sides gradually decreases. When α is 50°, the plastic zone area of the two sides is significantly smaller than that of the roof and the floor and the plastic zone is overall thin and highly elliptical. When α is 60°, distortion begins at the four corners of the plastic zone, and the butterfly plastic zone is gradually generated. The uneven malignant expansion occurs with the increase in the angle α.

Figure 12 shows the variation curve of the plastic zone size of the roadway with the axial angle α of the roadway. The following can be seen from the curve:

(1) When α is 0~60°, the maximum radius of the plastic zone in the rock surrounding the circular roadway occurs in the middle of the roadway roof. When α is 60–90°, the maximum size of the plastic zone of the surrounding rock occurs in the two roadway wings.

(2) When α is in the 0~40° range, the size of the plastic zone of the two roadway wings does not change much and is in a relatively stable stage. When α = 40°, the size of the plastic zone of the wing angle begins to increase sharply and the failure radii are 1.50, 1.68, 2.44, 3.32, 4.04, and 4.42 m, respectively. When the axial angle is 90°, the radius of the roadway plastic zone expands by 1.95 times.

(3) When the axial angle of roadway increases from 0° to 40°, the size of the plastic zone in the middle of roof decreases gradually. When α is 30°, the size of the plastic zone in the middle of the roof is the smallest, 1.50 m. From 40°, the depth of the plastic zone in the middle of the roof gradually increases, with the maximum value of 2.76 m, increasing by 0.84 times.

(4) Overall, the plastic zone size in the middle of the roadway decreases with the increase in the axial angle of the roadway. The size of the plastic zone is the largest at 0°, which is 1.74 m, and it is stable at 0.26 m at 40~80°. When α is 90°, the radius of the plastic zone in the sidewall increases slightly.

(5) In the σ_H-dominated stress field, with the increase in the axial angle α of the roadway, the size slope of the wing angle plastic zone shows high sensitivity. The curve slope changes greatly, followed by the sidewall curve slope, and the roof is the smallest. Therefore, in the σ_H-dominant stress field, the sensitivity of different positions of the roadway to angle α is wing angle > side > roof.

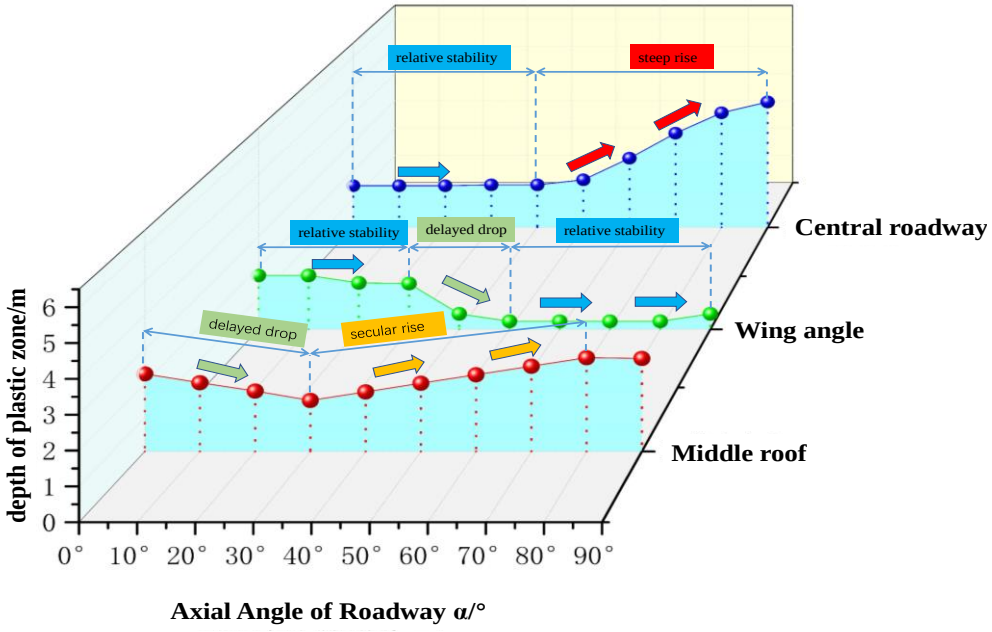

Figure 12. Variation in the depth of the plastic zone with axial angle α.

4. Comprehensive Analysis of the Orientation Criterion under Three Dominant Stress Fields

4.1. σ_{HZ}-Dominant Stress Field Orientation Criterion

In the σ_{HZ}-dominant stress field, it can be seen from the analysis in Section 2 that the roadway surrounding rock may be under four different stress environments, and the optimal orientation of the roadway in the rotation process is determined by the three principal stresses of the stress field. In the above numerical simulation scheme, the three principal stress values are introduced in Equation (9), and the optimal orientation angle is about 16°. From the numerical simulation results, it can be seen that the plastic zone size is slightly less than 16° when the roadway angle is about 40°. This is because the axial stress of the roadway has a certain effect on the size of the plastic zone but has little effect on the shape of the plastic zone of the surrounding rock. By determining the optimized angle, the butterfly hazard risk area is effectively avoided.

Therefore, in the σ_{HZ}-dominant stress field, according to the optimization angle formula, the orientation optimization angle can be obtained. In the neighborhood of the optimization angle, there is no butterfly stable area or butterfly hidden danger risk area.

4.2. σ_Z-Dominant Stress Field Orientation Criterion

In the σ_Z-dominant stress field, when α is 0°, the roadway is in a high-deviatoric-stress environment, which creates conditions for the formation of a butterfly plastic zone. With the increase in the axial angle α of the roadway, the confining pressure ratio gradually increases (close to 1), and the butterfly risk gradually decreases. When α is 90°, although the confining pressure ratio of the roadway is closest to 1, due to the influence of the axial stress of the roadway, the size of the plastic zone of roadway surrounding rock is slightly larger than 50° but the shape is slightly affected by axial stress, which is lateral ellipse and easy to support. When α is about 50°, the influence of the confining pressure ratio begins to increase, and the butterfly risk increases sharply with an increase in the angle.

Therefore, in the σ_Z-dominant stress field, the roadway is a butterfly-free stable area within the 50~90° range, and the requirements for the surrounding rock support of the roadway are not high. In the 0~40° range, it is a butterfly-shaped risk area, where it is difficult to provide support and there is a high risk of roof fall.

4.3. σ_H-Dominant Stress Field Orientation Criterion

In the σ_H-dominated stress field, when the axial angle α of the roadway is 0°, the confining pressure ratio of roadway surrounding rock is the smallest. With an increase in the axial angle α of the roadway, the confining pressure ratio gradually increases, and a high-deviatoric-stress-environment area gradually forms. When α is 0°, although the confining pressure ratio of the roadway is the smallest, the size of the plastic zone in rock surrounding the circular roadway is slightly larger than 40° due to the influence of the axial stress of the roadway, but this stress has little effect on the shape of the plastic zone, only on the size. When α is about 40°, the influence of the axial stress of the roadway on the size of the plastic zone decreases and the influence of the confining pressure ratio begins to increase. With an increase in angle α, high deviatoric stress leads to the formation of a butterfly plastic zone.

Therefore, in the σ_H-dominated stress field, different from maximum horizontal stress theory, the roadway is a butterfly-free stable region in the 0~40° range, which is conducive to roadway maintenance. In the 50~90° range, it is a butterfly-shaped risk area, which is not conducive to roadway maintenance.

5. Guidance to Engineering Practice

It can be seen from the above analysis that the roadway layout direction under different stress fields influences the deformation and failure of roadway surrounding rock and the different layout directions of the roadway have an important effect on the stress state of roadway surrounding rock. When the stress state of the roadway is under the condition of a high confining pressure ratio, the roadway surrounding rock will produce butterfly failure, and the butterfly plastic zone has an important influence on the stability of roadway surrounding rock. This study can guide engineering practice from the following three aspects:

(1) For mine production preparation, as far as possible, use the analysis method in this paper for the layout directions of the return airway, the transportation roadway, the contact roadway, and some chambers to avoid the high confining pressure ratio stress field of roadway and chamber. Before excavating the roadway, the stability of surrounding rock in different directions of the roadway should be analyzed based on the test results of ground stress. According to the test results of ground stress, the plastic zone should be circular or elliptical so as to avoid the formation of a butterfly plastic zone.

(2) When the roadway is in a different stress environment, the shape and size of the plastic zone of the roadway can be obtained according to the ground stress data of the mine and the above theoretical analysis, the stability of the surrounding rock of the roadway can be evaluated theoretically, and the surrounding rock can be supported in a targeted manner according to different plastic zone shapes.

(3) When the roadway or chamber is inevitably arranged in the range of a high confining pressure ratio due to the influence of production replacement or geological structure (such as faults) in the process of roadway layout, the butterfly plastic zone should be strengthened according to the above analysis and the parts where the butterfly leaf is easy to expand should be strengthened.

6. Discussion

Based on the butterfly failure theory of roadway surrounding rock, this paper studied the evolution law and orientation criterion of the plastic zone in rock surrounding a circular roadway under different stress fields, providing theoretical guidance for optimal roadway layout. Based on the theory, the description method, and the technology used in this paper, there are still some problems to be solved, and further research and learning are needed in the following aspects:

(1) Due to the large depth, the in situ stress field environment of a deep roadway becomes complex, reflected not only in the size but also in the direction of the stress, which

will change to different degrees. In this paper, only the size of the stress vector was analyzed, not the change in the stress direction. Next, it is necessary to analyze the evolution law and orientation criterion of the roadway plastic zone under different deflection angles.

(2) In the study of the plastic zone size of roadway surrounding rock, the solution of the plastic zone boundary equation under a three-dimensional stress field is complex. Therefore, this paper adopted the 8-order implicit equation of a butterfly plastic zone, which is based on the Mohr–Coulomb criterion and does not consider the influence of the roadway axial stress on the plastic zone size of roadway surrounding rock. In the next step, it is necessary to further analyze the size of the plastic zone under a three-dimensional stress field to study the influence of axial stress of the roadway on the stability of the surrounding rock.

7. Conclusions

(1) The original rock stress field is mainly divided into the σ_{HZ}-dominant stress field, the σ_Z-dominant stress field, and the σ_H-dominant stress field. Under different dominant stress fields, the angles between the axial direction of the roadway and the direction of the maximum horizontal principal stress are different, and the degree of damage of the surrounding rock of the roadway is different. When the axial direction of the roadway is consistent with the direction of the maximum horizontal principal stress, the stability of the surrounding rock of the roadway is not necessarily good, and it may be in the butterfly risk area, which is different from the maximum horizontal stress theory.

(2) According to the butterfly failure theory of roadway surrounding rock, the stability of roadway surrounding rock with different axial angles under three different dominant stress fields is analyzed theoretically. The stress environment under different dominant stress fields is classified, and each stress field is divided into four stress environments.

(3) The theoretical analysis results show that in the σ_{HZ}-dominant stress field, the shape of the plastic zone changes from elliptical to quasi-circular to butterfly, and the difference between the maximum and minimum plastic zone sizes is 2.52 m; in the σ_Z-dominant stress field, the shape of the plastic zone transitions from butterfly to ellipse, and the difference between the maximum and minimum plastic zone sizes is 3.31 m; and in the σ_H-dominant stress field, the shape of the plastic zone transitions from ellipse to butterfly, and the difference between the maximum and minimum plastic zone sizes is 1.60 m.

(4) The numerical simulation results show that in the σ_{HZ}-dominant stress field, the optimized angle range of roadway orientation is determined by three principal stresses. In the σ_Z-dominant stress field, the optimized angle range of roadway orientation is 50~90° and the butterfly hidden danger zone is in the 0~50° range; in the σ_H-dominated stress field, the optimized angle range of roadway orientation is 0~40° and 50~90° is the hidden danger zone.

Author Contributions: Conceptualization, H.L., Z.H. (Zijun Han), Z.H. (Zhou Han) and X.G.; methodology, Z.H. (Zijun Han) and T.H.; software, S.W.; validation, Z.L. and T.H.; formal analysis, Z.H. (Zhou Han) and S.W.; investigation, Z.H. (Zhou Han) and X.G.; data curation, Z.H. (Zijun Han), J.M. and Z.L.; writing—original draft preparation, Z.H. (Zijun Han) and Z.H. (Zhou Han); writing—review and editing, Z.L. and S.W.; supervision, H.L.; funding acquisition, H.L. All authors have read and agreed to the published version of the manuscript.

Funding: This research was funded by the National Natural Science Foundation of China, grant numbers 51774288, 52004289).

Acknowledgments: The authors are thankful to the anonymous reviewers for their kind suggestions.

Conflicts of Interest: The authors declare no conflict of interest.

References

1. Qian, M.G.; Shi, P.W.; Xu, J.L. *Mining Pressure and Strata Control*; China University of Mining and Technology Press: Xuzhou, China, 2010. (In Chinese)
2. Ma, N.J.; Hou, C.J. *The Theory and Application of Mining Roadway Pressure*; China University of Mining and Technology Press: Xuzhou, China, 1995; pp. 82–91. (In Chinese)
3. Zhao, H.B.; Cheng, H.; Wang, L. The distribution characteristics of deviatoric stress field and failure law of surrounding rock under non-hydrostatic pressure. *Coal J.* **2021**, *46*, 370–381.
4. Wang, W.J.; Han, S.; Dong, E.Y. Boundary equation of plastic zone in roadway surrounding rocks considering supporting effect and its. *J. Min. Saf. Eng.* **2021**, *38*, 749–755.
5. Li, C.; Zhang, W.L.; Wang, N.; Cheng, H. Roof stability control based on plastic zone evolution during mining. *J. Min. Saf. Eng.* **2019**, *36*, 753–761.
6. Wang, J.C.; Wang, Z.H.; Yang, J.; Tang, Y.S.; Li, B.B.; Meng, Q.B. Mining-induced stress rotation and its application in longwall face with large length in kilometer deep coal mine. *J. Coal* **2020**, *45*, 876–888.
7. Kang, H.P.; Jiang, P.F.; Gao, F.Q.; Wang, Z.Y.; Liu, C.; Yang, J.W. Analysis on stability of rock surrounding heading faces and technical approaches for rapid heading. *J. Coal* **2021**, *46*, 2023–2045.
8. Behnam, B.; Fazlollah, S.; Hamid, M. Prediction of plastic zone size around circular roadways in non-hydrostatic stress field. *Int. J. Min. Sci. Technol.* **2014**, *24*, 81–85. [CrossRef]
9. Xu, M.F.; Wu, S.C.; Gao, Y.T.; Ma, J.; Wu, Q.L. Analytical elastic stress solution and plastic zone estimation for a pressure-relief circular roadway using complex variable methods. *Roadwayling Undergr. Space Technol.* **2018**, *84*, 381–398. [CrossRef]
10. Hou, C.J. Key Technologies for Surrounding Rock Control in Deep Roadway. *J. China Univ. Min. Technol.* **2017**, *46*, 970–978.
11. Ma, N.J.; Li, J.; Zhao, Z.Q. Distribution of deviatoric stress field and plastic zone in circular roadway surrounding rock. *J. China Univ. Min. Technol.* **2015**, *44*, 206–213.
12. Chen, D.H.; Hua, X.Z. Impact of In-situ Stress on Layout Direction of Deep Typical Gateways. *J. Undergr. Space Eng.* **2018**, *14*, 1122–1129.
13. Sun, Y.F. Affect of horizontal stress on stability of roadway surrounding rock. *J. Coal* **2010**, *35*, 891–895.
14. Wu, X.Y.; Liu, H.T.; Li, J.W.; Guo, X.F.; Lv, K.; Wang, J. Temporal-spatial evolutionary law of plastic zone and stability control in repetitive mining roadway. *J. Coal* **2020**, *45*, 3389–3400.
15. Zhao, Z.Q.; Ma, N.J.; Liu, H.T.; Guo, X. A butterfly failure theory of rock mass around roadway and its application prospect. *J. China Univ. Min. Technol.* **2018**, *47*, 969–978.
16. Guo, X.F.; Ma, N.J.; Zhao, X.D.; Zhao, Z.Q.; Li, Y.-E. General shapes and criterion for surrounding rock mass plastic zone of round roadway. *Coal J.* **2016**, *41*, 1871–1877.
17. Kang, H.P.; Wang, J.H. *Coal Roadway Bolt Support Theory and Complete Set of Technology*; Coal Industry Press: Beijing, China, 2007.
18. Hao, Z.; Guo, L.F.; Zhao, X.; Cheng, G.X.; Zhang, G.H. Analysis of burst failure energy characteristics of mining roadway surrounding rock. *Coal J.* **2020**, *45*, 3995–4005.
19. Zhao, Z.Q. *Study on Deformation and Failure Mechanism and Control Method of Surrounding Rock of Large Deformation Mining Roadway*; China University of Mining and Technology: Beijing, China, 2014.
20. Guo, X.F. *Determination Criteria and Application of Plastic Zone Morphology of Roadway Surrounding Rock*; China University of Mining and Technology: Beijing, China, 2019.
21. Sun, X.F. *Materials Mechanics*, 4th ed.; Higher Education Press: Beijing, China, 2002. (In Chinese)